



Betulinic acid arrests cell cycle at G2/M phase by up-regulating metallothionein 1G inhibiting proliferation of colon cancer cells

Sen Wang^{a,b,1}, Yuqin Zhang^{c,1}, Xiaxia Yang^a, Kexin Wang^d, Xiao Yang^a,
Baogui Zhang^e, Bin Zhang^{a,f}, Qingli Bie^{a,b,*}

^a Department of Laboratory Medicine, Affiliated Hospital of Jining Medical University, Jining Medical University, Jining, Shandong, China

^b Postdoctoral Mobile Station of Shandong University of Traditional Chinese Medicine, Jinan, Shandong, China

^c Blood Transfusion Department, Affiliated Hospital of Jining Medical University, Jining Medical University, Jining, Shandong, China

^d Department of Radiology, Affiliated Hospital of Jining Medical University, Jining Medical University, Jining, Shandong, China

^e Gastrointestinal Surgery, Affiliated Hospital of Jining Medical University, Jining Medical University, Jining, Shandong, China

^f Institute of Forensic Medicine and Laboratory Medicine, Jining Medical University, Jining, Shandong, China

ARTICLE INFO

Keywords:

Betulinic acid
Colon cancer
RNA sequencing
Cell cycle
MT1G

ABSTRACT

Betulinic acid (BA) is a pentacyclic triterpene found in many plant species and has a broad-spectrum anti-tumor effect in various cancers, including colon cancer (CRC). However, its anti-cancer mechanism in CRC is no clear. RNA sequencing and bioinformatics analysis showed BA up-regulated 378 genes and down-regulated 137 genes in HT29 cells, while 2303 up-regulated and 1041 down-regulated genes were found in SW480 cells. KEGG enrichment analysis showed BA significantly stimulated the expression of metallothionein 1 (MT1) family genes in both HT29 and SW480 cells. Metallothionein 1G (MT1G) was the gene with the highest upregulation of MT1 family genes induced by BA dose-dependently. High MT1G expression enhanced the sensitivity of CRC cells to BA, whereas, MT1G knockdown had the opposite effect in vitro and in vivo. GSEA and GSCA showed genes affected by BA treatment were involved in cell cycle and G2/M checkpoint in CRC. Flow cytometry further exhibited BA reduced the percentage of G0/G1 cells and increased the percentage of G2/M cells in a dose-dependent manner, which could be rescued by MT1G knockdown. Moreover, MT1G also counteracted the BA-induced changes in cell cycle-related proteins (CDK2 and CDK4) and p-Rb. In summary, we have revealed a new anti-tumor mechanism that BA altered the cell cycle progression of CRC cells by upregulating MT1G gene, thereby inhibiting the proliferation of CRC cells.

1. Introduction

Colon cancer (CRC) is the fourth leading cause of cancer death worldwide [1]. The 5-year and 10-year survival rates are 65 % and 58 %, respectively [2]. Drug resistance is a common feature of many patients with CRC and find new drugs with new anticancer mechanisms is an effective method to improve the survival of patients with CRC. The advantage of traditional Chinese medicines (TCMs) over small molecule targeted agents for the treatment of chronic illnesses is multifold [3]. In recent years, many monomer

* Corresponding author. Department of Laboratory Medicine, Affiliated Hospital of Jining Medical University, 89 Guhuai Road, Jining 272000, China.

E-mail address: xiaobie890101@163.com (Q. Bie).

¹ Contributed equally.

<https://doi.org/10.1016/j.heliyon.2023.e23833>

Received 5 June 2023; Received in revised form 11 December 2023; Accepted 13 December 2023

Available online 29 December 2023

2405-8440/© 2023 The Authors. Published by Elsevier Ltd. This is an open access article under the CC BY-NC-ND license (<http://creativecommons.org/licenses/by-nc-nd/4.0/>).

components which is target of TCM have been gradually revealed, laying a foundation for its clinical application.

Betulinic acid, BA, is a naturally occurring pentacyclic lupin-type triterpenoid and its monomer components is mainly isolated from birch trees with a wide range of biological effects, including antiviral, antiparasitic, antibacterial, and anti-inflammatory activities. In addition, BA has a prominent site of natural anticancer drugs without toxicity to normal cells in vitro and in vivo [4]. BA was attenuated as a potentially selective anti-melanoma agent and entered a phase II clinical trial for skin cancer [5]. Lactoferrin-tethered betulinic acid nanoparticles promoted rapid delivery and cell death in triple negative breast and laryngeal cancer cells [6]. BA suppressed breast cancer aerobic glycolysis via caveolin-1/NF-kappaB/c-Myc pathway [7]. BA suppressed ovarian cancer cell proliferation through induction of apoptosis [8]. BA delivered in liposomes reduces growth of colon cancers in mice without causing systemic toxicity [9]. BA was reported as potential antitumor agents [10]. Therefore, BA inevitably inhibited cancer cell proliferation by important mechanism. Today, transcriptome analysis offers the opportunity to analyze a large number of targets and determine mechanisms of action. However, the specific mechanism driving BA anti-tumor in CRC using RNA sequencing method remains unclear.

MT plays an important role in tumorigenesis, progression and drug resistance [11]. Most of the biological functions of MTs are related to detoxification of heavy metals and metal binding of enzymes and transcription factors zinc/copper [12]. MT1G is a member of the metallothionein family, MT1G promotes the chemosensitivity of CRC cells [13], functions as a novel biomarker correlated with prognosis and immune infiltration in CRC [14]. MT1G also plays a vital role in the change from G1 to S in the growth of acute leukemia cells [15]. However, whether MT1G is involved in BA-induced proliferation inhibition remains to be further studied.

In this paper, RNA sequencing was used to screen the differentially expressed genes (DEGs) induced by BA in CRC cells, and the functions of these DEGs were analyzed through bioinformatics analysis. The results showed that 263 was differentially transcribed after BA treatment in both SW480 and HT29 CRC cells. Gene Ontology (GO) and Kyoto Encyclopedia of Genes and Genomes (KEGG) analysis revealed that these DEGs were significantly enriched in mineral absorption and the cell cycle. Among these DEGs, five MT family proteins were all significantly activated by BA. Notably, MT1G was the most upregulated. Therefore, we used MT1G gene as the main research objects to explore whether BA depends on this protein to inhibit proliferation of colon cells.

2. Materials and methods

2.1. Cell culture and sample collection

BA (CAS# HY-10529) was purchased from Med Chem Express and purity was greater than 98 %. 1 mg BA was dissolved to 1 mL DMSO, and then the BA solutions were diluted into the complete medium to reach the indicated concentrations. The human CRC cell lines HT29 and SW480 were purchased from National Collection of Authenticated Cell Cultures and authenticated by Shanghai Yihe Applied Biotechnology Co., Ltd. HT29 was cultured with McCoy's 5A medium and SW480 was cultured with DMEM medium, both of which were supplemented with 10 % fetal bovine serum (GIBCO No.: 10099141) and 1 % penicillin/streptomycin (Sigma).

2.2. RNA extraction

2×10^6 SW480 and HT 29 cells were seeded into 6-well plates and cultured for 24h. After adding 100 μ M or 80 μ M BA and the same concentration of control DMSO to the medium for 24h, removing the supernatant and adding 500 μ l Buffer RL directly to the plate for digestion, lysis, and vortex shaking until no obvious cell mass was present. The split samples were transferred to FastPure gDNA-Filter Columns III (FastPure gDNA-Filter Columns III already in the collection tube) and centrifuged at 12,000 rpm for 30 s. The FastPure gDNA-Filter Columns III was discarded and the filtrate was collected. 0.5 \times the filtrate volume of absolute ethanol was added to filtrate. Add 700 μ l Buffer RW1, 12,000 rpm to the FastPure RNA Columns III by centrifugation for 30 s and the filtrate was discarded. 700 μ l Buffer RW2, 12,000 rpm for 30 s and the filtrate was discarded. Add 500 μ l Buffer RW2 (absolute ethanol) added to FastPure RNA Columns III, centrifuge at 12,000 rpm for 2 min and carefully remove the adsorption column from the collection tube. Carefully, the adsorption column was transferred to a new RNase-free Collection Tubes 1.5 mL centrifuge tube, dropping 50–200 μ l of RNase-free ddH₂O to the central adsorption column, standing at room temperature for 1 min, centrifugation at 12,000 rpm for 1 min to elute RNA. The extracted Total RNA can be used directly for downstream experiments or stored from -85 to -65 °C.

2.3. mRNA library construction, filtering and reference genome alignment

mRNA library construction was performed by BGI company [16]. The filtering software SOAP nuke independently developed by BGI for filtering was used [17]. Hierarchical indexing for spliced alignment of transcripts software was used compare reference genomes.

2.4. DEGs screening and hierarchical clustering analysis

The PoissonDis method [18] was used to identify the DEGs between BA treated and control samples, $|\log_2FC| > 1$, adjusted False discovery rate (FDR) < 0.001 is used as the threshold to identify DEGs. Based on the detection results of DEGs, the hierarchical cluster analysis of the coupled DEGs was performed using the R-pack heatmap.

2.5. GO and KEGG pathway analysis

GO, KEGG and Reactome were used as bioinformatic tool that provides the comprehensive information to calculate the *P* value, and then the *P* value was corrected by FDR. Function of *Q* value ≤ 0.05 was considered to be a significant enrichment.

2.6. RT-PCR

The Evo M-MLV RT kit with gDNA clean for RT-PCR (AG11711) was employed for reverse transcription. RT-PCR was conducted using the Takara SYBR® Premix Ex Taq™ II (Tli RNaseH Plus) kit (RR820Q) as per the provided guidelines to assess the relative expression of the beta-actin, MT1G genes, as well as other genes. The primer sequences of the 17 genes were shown in [Supplementary Table 1](#). The experiment was repeated 3 times.

2.7. MT1G knockdown and over-expression assay

The RNAi lentiviral vectors LV-MT1G-RNAi and control group LV-NC-RNAi, the MT1G lentivirus over-expression group pLV [Exp]-EGFP:T2A:Puro-EF1A > hMT1G and the control group pLV[Exp]-EGFP:T2A:Puro-EF1A > mCherry were respectively constructed and packaged by Shanghai Genechem. The knockdown (shMT1G) and control (shNC) group targeted sequences were “5'-GCTCCCAAGTACAAATAGAGT-3'” and “5'-TTCTCCGAACGTGTCACGT-3'”, respectively, while the sequence of the MT1G gene (NM_001301267.1) was over-expressed. Before infection, the virus was slowly thawed on ice. The original medium was aspirated from the cells, 1/2 volume of fresh medium was added, the virus stock solution was added to the cells, and the cells were mixed gently. Small volumes were infected at 37 °C for 4 h, and the medium was replenished to a normal volume after 4 h. After 24 h of infection, the medium was replaced with fresh complete culture medium, and cultured at 37 °C for 48 h. The GFP expression efficiency was observed by fluorescence microscopy. The medium was replaced with fresh complete medium containing puromycin, and the stably transduced cell line was screened.

2.8. Cell proliferation assay

We used two types of cell lines in this study, including SW480 and HT29 (All cell lines were uniformly validated by STR). MT1G over-expressed SW480 cells or MT1G knock down HT29 cells and control cells were seeded in a 96-well plate (10000 per well) for 24h, and then treated with BA at different concentrations and control (isometric DMSO) for another 24h with 5 repeats. 10 μ l of Cell counting kit 8 (CCK8) reagent was added to each well and incubated at 37 °C for 1h. The absorbance value was measured at 490 nm by using a Biotek Synergy H1 Full-featured Microplate Reader. Cell survival rate was statistically analyzed using GraphPad Prism 8 software.

2.8.1. Cell cycle assays

To analyze the cell cycle, 2×10^6 cells infected with shMT1G or shNC lentivirus were inoculated into the 6-well plates for 24h, and treated with BA at 100 μ M or 80 μ M and control (isometric DMSO) for another 24h, and then cells were collected, washed three times in PBS, and fixed in 70 % ice ethanol for 4 h or overnight. The cells were resuspended with the directed dilution method followed by a propionil iodide solution (50 μ g/mL propidium iodide, 50 μ g/mL RNase A) (Mocon Biotechnology, MX3222). The cell cycle was analyzed based on the flow cytometry by flow cytometry (BD Bioscience, NJ).

2.9. Western blotting

Western blotting was performed as described previously [19]. CDK2 (#2546), CDK4 (#12790), phospho-Rb (Ser807/811) (#8516T), Rb (#9313) and anti-rabbit IgG, HRP-linked antibody (#7074) were purchased from CST. MT1G (#OM263051) was purchased from OmnimAbs. Beta Actin Ab polyclonal antibody (#AF7018) was purchased from Affinity Biosciences.

2.10. GSEA and GCEA analysis of BA-induced DEGs

GSEA, a computational method that determines whether an a priori defined set of genes shows statistically significant, concordant differences between two biological states. The Molecular Signatures Database (MSigDB) was used with GSEA software. Enter gene pairs in the investigate dialog box, select H: hallmark gene sets, and calculate overlapping genes. GSCAonline software was used to validate gene enrichment information in 329 (COAD) Colon adenocarcinoma samples (Tumor:288; Normal:41; paired:26), GSVA & Pathway activity was explored. *, *P* value ≤ 0.05 ; #, *FDR* ≤ 0.05 .

2.10.1. Xenograft experiments in mice

All animal experiments received approval from the Animal Ethics Committee of Jining Medical College (Approval No. 2022B060). Four-week-old male BALB/c nude mice and NVSG mice, the internationally recognized tool mice with the highest degree of immunodeficiency, were purchased from Jinan Pengyue Experimental Animal Breeding Co., LTD. The mice were subcutaneously administered with either 1×10^7 MT1G knock down cells or control SW480 cells, with each group consisting of five mice, after 7 days, BA (20 mg/kg, 40 mg/kg, 80 mg/kg) was intraperitoneally injected into these mice every day for 1 month. The mice were housed with a

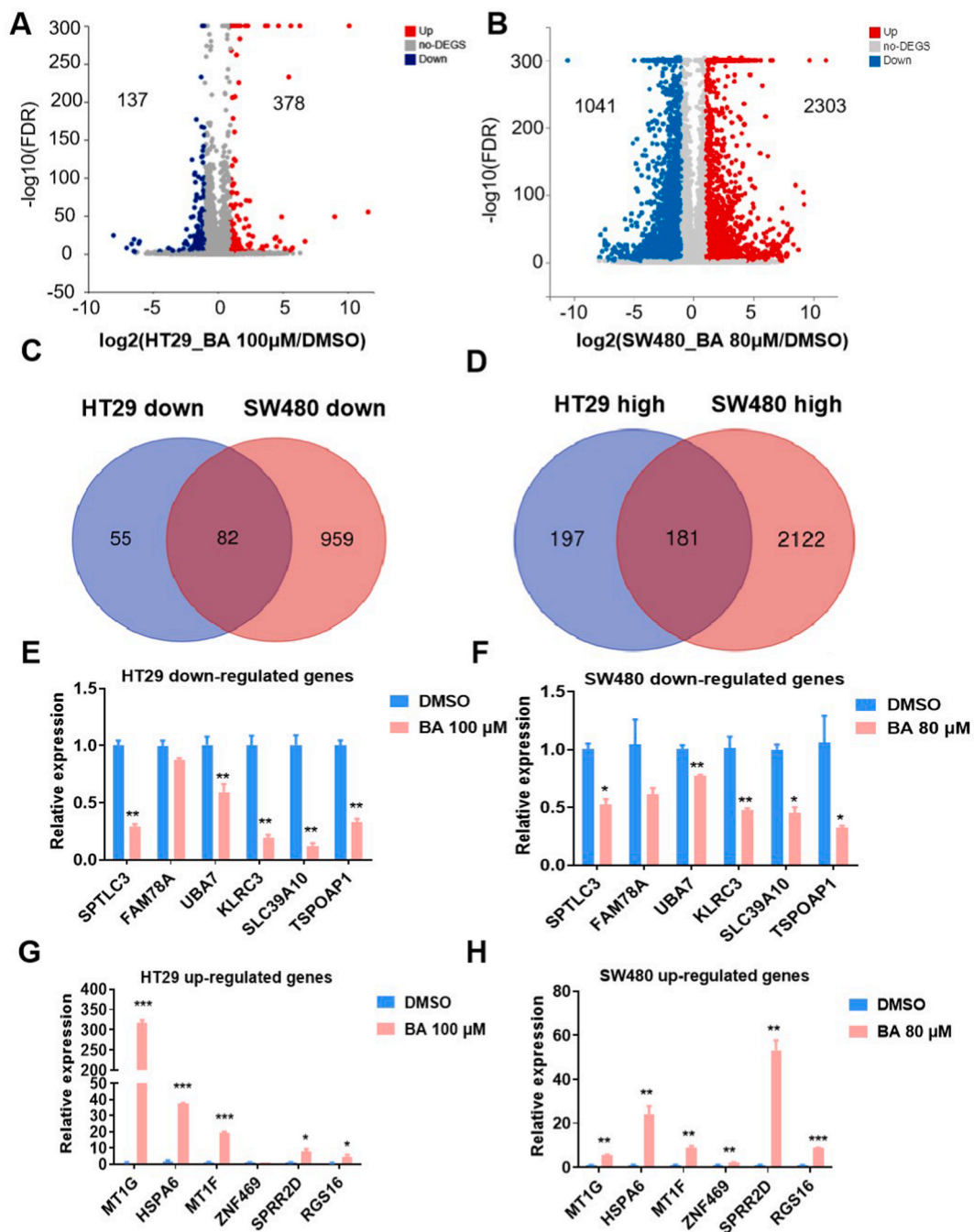


Fig. 1. BA-induced DEGs analysis in HT29 and SW480 cells. A and B. Volcano map of DEGs (>2 fold change) in HT29 and SW480 cells treated with BA at 100 μ M or 80 μ M for 24 h. The X axis represents the difference multiple value after \log_2 conversion, and the Y axis represents the significance value after $-\log_{10}$ conversion. Red represents upregulated DEGs, blue represents downregulated DEGs, and gray represents non-DEGs. Student's *t*-test: $P < 0.05$, FDR value < 0.001 , $n = 5$. C and D. Venn diagram of the overlapping highly regulated and downregulated genes in SW480 and HT29 cells treated with BA for 24 h. E-H. SW480 and HT29 cells were treated with BA at the indicated concentrations for 24 h and the cells were collected for RT-PCR using indicated primers. GAPDH was used as an internal control. Data are presented as the mean \pm SD, $n = 3$, * $P < 0.05$, ** $P < 0.01$, *** $P < 0.001$, **** $P < 0.0001$.

12-h light/dark cycle. All procedures strictly adhered to established guidelines. Ultimately, the mice were euthanized with CO₂, and the resultant tumor samples were subjected for weighing and statistical analysis.

2.11. Statistical analysis

The data were used as an average, and the standard deviation (SD). The results were statistically analyzed using GraphPad Prism 8 software. Student's T test and two-way ANOVA were used. * $P < 0.05$, ** $P < 0.01$, *** $P < 0.001$ and **** $P < 0.0001$ were considered to have low, medium, and high statistical significance, respectively.

3. Results

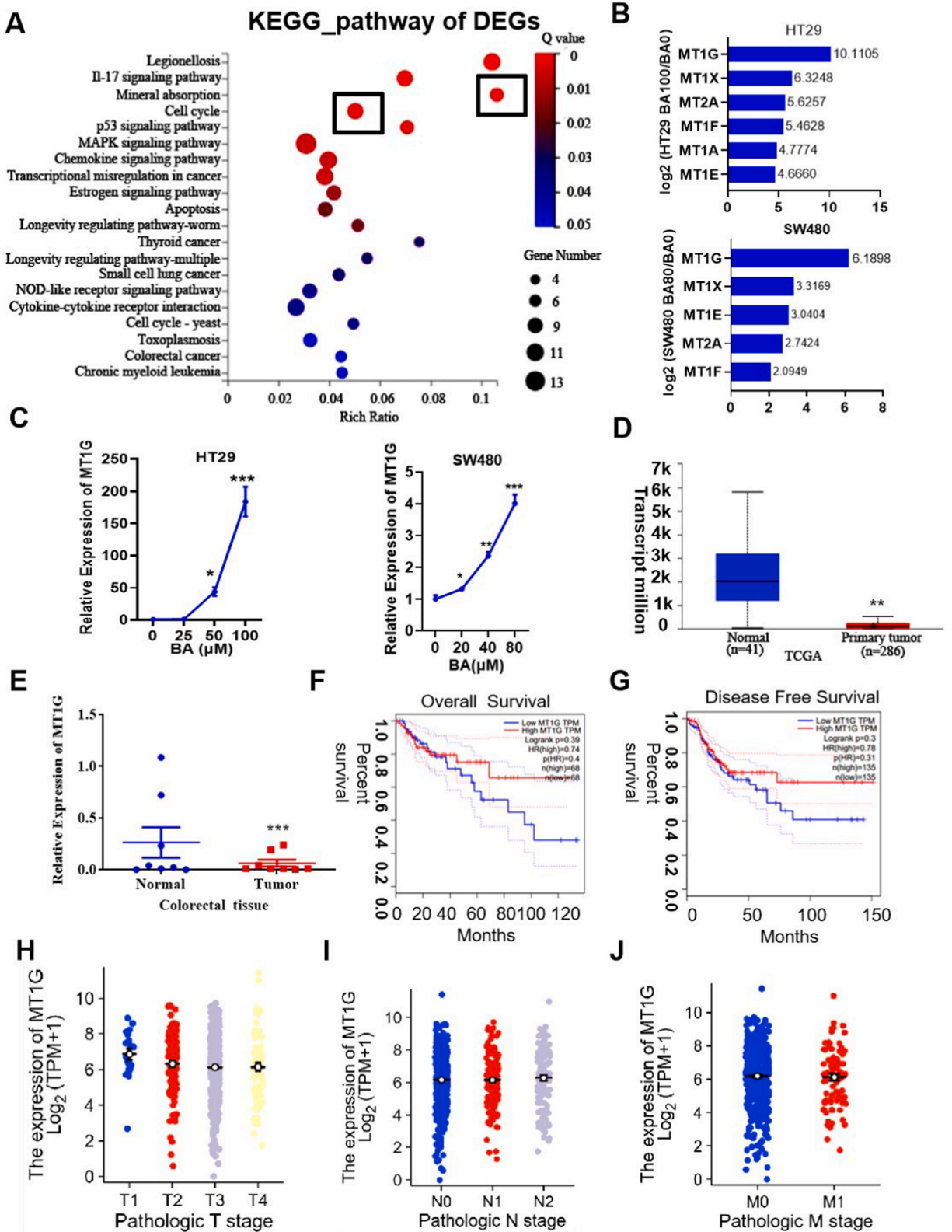
3.1. RNA sequence analysis of human colorectal cancer cells with or without BA

To study the gene expression profile of human colorectal cancer cells treatment with BA, HT29 and SW480 cells were treated with BA and DMSO for 24h at indicated concentration. Our previous research has confirmed that the IC₅₀ values of HT29 and SW480 was 100 μ M or 80 μ M after treatment for 24h, respectively [19]. Therefore, we chose the concentration corresponding to the IC₅₀ value in this study. RNA sequencing analysis identified 515 and 3344 differentially expressed mRNAs (>2 fold change, FDR value < 0.05) in HT29 or SW480 cells treated with BA at 100 μ M or 80 μ M or DMSO for 24h, respectively. There were 378 up-regulated and 137 down-regulated mRNAs in HT29 cells and 2303 up-regulated and 1041 down-regulated mRNAs in SW480 cells (Fig. 1A and B). Venn diagram analysis showed 181 genes were highly-expressed, and 82 genes were down-expressed in both HT29 and SW480 cells under BA treatment (Fig. 1C and D). Hierarchical cluster analysis of DEGs in SW480 or HT29 cells is displayed in the heatmap

Table 1

The top 20 up-regulated and 20 down-regulated genes in both SW480 and HT29 cells.

Gene Symbol	SW480		HT29	
	log2 (BA80/Ctr)	FDR (BA80/Ctr)	log2 (BA100/Ctr)	FDR (BA100/Ctr)
CRYAB	4.04	<0.001	4.51	<0.001
BHLHA15	3.99	<0.001	1.95	<0.001
ARC	4.56	<0.001	1.60	<0.001
BPIFC	7.02	<0.001	2.40	<0.001
GEM	5.29	<0.001	1.25	<0.001
CXCL1	4.06	<0.001	1.31	<0.001
CXCL2	4.89	<0.001	1.66	<0.001
CXCL3	6.66	<0.001	2.70	<0.001
HSPA1A	4.55	<0.001	1.48	<0.001
HSPA1B	4.17	<0.001	1.30	<0.001
HSPA6	11.05	<0.001	3.67	<0.001
CXCL8	9.22	<0.001	2.46	<0.001
KRT16	4.91	<0.001	3.44	<0.001
MT1G	6.19	<0.001	10.11	<0.001
ANGPTL4	3.97	<0.001	4.52	<0.001
CCL20	5.36	<0.001	3.28	<0.001
SPRR2D	4.39	<0.001	3.76	<0.001
TNFAIP3	5.60	<0.001	2.03	<0.001
UPP1	4.84	<0.001	1.24	<0.001
SEMA7A	4.24	<0.001	1.62	<0.001
SEMA3A	-2.91	<0.001	-1.85	<0.001
IQGAP2	-2.80	<0.001	-1.26	<0.001
LRRC45	-2.89	<0.001	-1.03	<0.001
PLA2R1	-3.04	<0.001	-1.41	<0.001
RAB26	-3.20	<0.001	-1.34	<0.001
HPGD	-2.81	<0.001	-1.09	<0.001
GLDN	-3.27	<0.001	-1.71	<0.001
KLRC3	-2.84	<0.001	-6.41	<0.001
SP5	-2.85	<0.001	-1.08	<0.001
FAM183A	-3.59	<0.001	-1.91	<0.001
C21orf58	-3.24	<0.001	-1.55	<0.001
SLC39A10	-2.87	<0.001	-2.40	<0.001
VANGL2	-3.83	<0.001	-1.32	<0.001
NYNRIN	-3.54	<0.001	-1.36	<0.001
SERF1A	-4.64	<0.001	-1.78	<0.001
SORBS2	-3.76	<0.001	-1.01	<0.001
LGR5	-4.00	<0.001	-1.77	<0.001
TNFSF10	-4.77	<0.001	-2.12	<0.001
SYT8	-4.64	<0.001	-1.54	<0.001
MGAM2	-3.17	<0.001	-1.30	<0.001

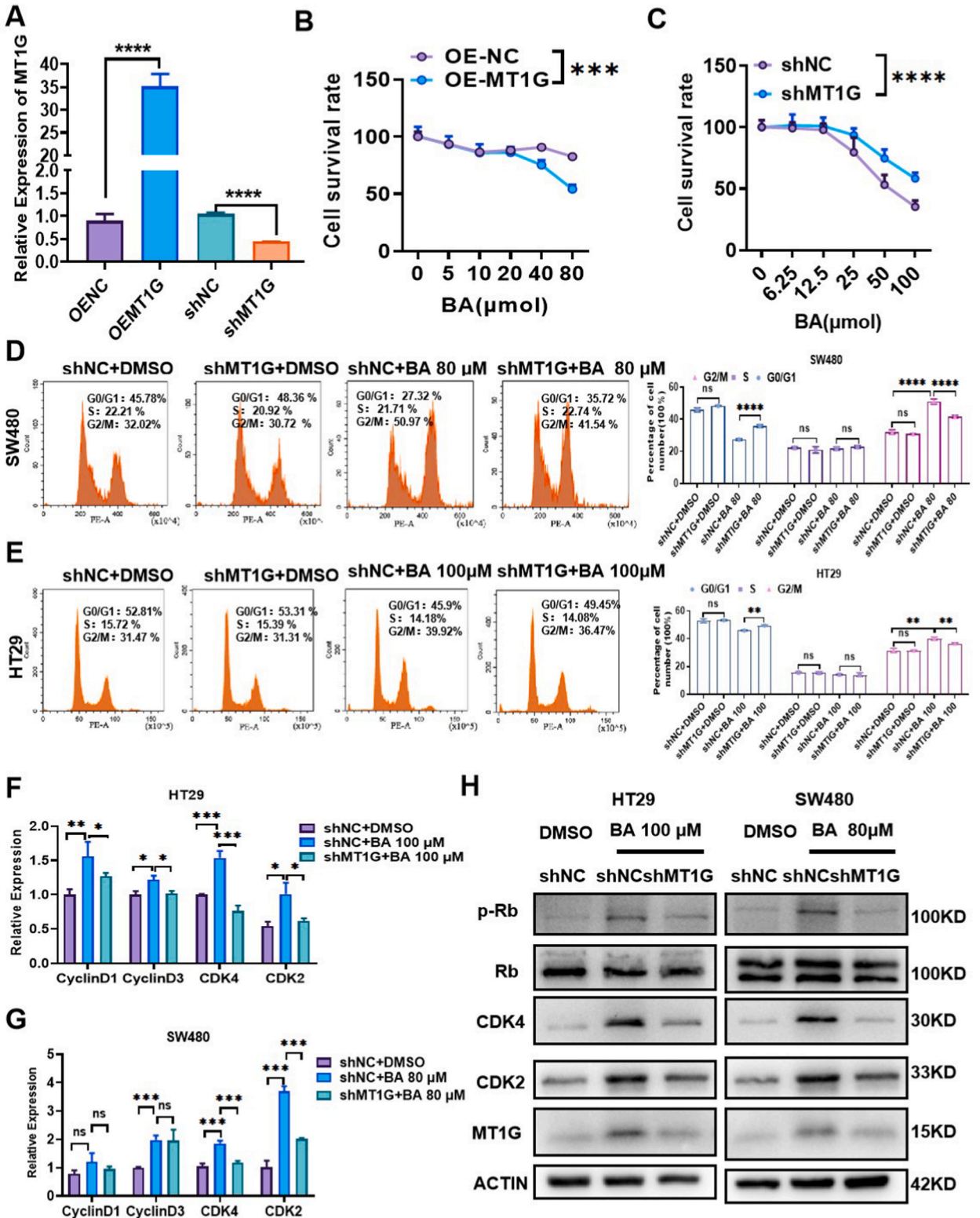


(caption on next page)

Fig. 2. BA promoted the expression of MT1G and MT1G was low expressed in colorectal cancer. **A.** According to the KEGG_pathway annotation classification, the phyper function in R software was used to perform enrichment analysis, calculate the *P* value, and then perform FDR correction on the *P* value to obtain the *Q* value. Generally, a function with a *Q* value ≤ 0.05 was regarded as significantly enriched. **B.** The expression of MT1G and other MT1 family genes was determined by RNA sequencing in both HT29 cells and SW480 cells after treatment with BA at 100 μ M or 80 μ M. Data are presented as the mean, *n* = 5. **C.** The expression of MT1G genes was further detected by RT-PCR in both SW480 cells and HT29 cells after treatment with BA at the indicated concentration. Data are presented as the mean \pm SD, *n* = 3, Student's *t*-test **P* < 0.05, ***P* < 0.01, ****P* < 0.001, *****P* < 0.0001. **D.** MT1G expression levels in colorectal cancer and normal patients were calculated by using GEPIA online. **E.** The mRNA levels of MT1G were analyzed by RT-PCR in 8 pairs of colorectal cancer and adjacent nontumor tissues (*n* = 8), which were collected from Jining Medical University Affiliated Hospital. Data are presented as the mean \pm SD, *n* = 3, Student's *t*-test, **P* < 0.05, ***P* < 0.01, ****P* < 0.001, *****P* < 0.0001. **F.** Kaplan-Meier curves of patients with colorectal cancer with low versus high expression of MT1G using TCGA sequencing data. GEPIA online software was used to analyze the relationship of MT1G gene with CRC patients' survival. **G.** Disease free survival of patients with colorectal cancer with low versus high expression of MT1G using TCGA sequencing data. GEPIA online software was used to analyze the relationship of MT1G gene with CRC patients' disease free survival. **H-J.** Association between MT1G expression and TNM stage in colorectal cancer patients by analyzing TCGA sequencing data. GEPIA online software was used to analyze the relationship of MT1G gene with CRC patients' TNM stage.

Table 2
GSEA analysis of overlapping DEGs induced by BA in CRC cells.

Gene Set Name	# Genes		k/K	p-value	FDR q-value
	Gene Set (K)	in Overlap (k)			
HALLMARK_G2M_CHECKPOINT	200	24	0.12	1.58E-23	7.92E-22
POINT					
HALLMARK_MITOTIC_SPINDLE	199	23	0.1156	3.27E-22	8.17E-21
HALLMARK_TNFA_SIGNALING_VIA_NFKB	200	17	0.085	1.77E-14	2.95E-13
HALLMARK_E2F_TARGETS	200	14	0.07	5.19E-11	6.49E-10
HALLMARK_HYPOXIA	200	11	0.055	7.55E-08	6.29E-07
HALLMARK_P53_PATHWAY	200	11	0.055	7.55E-08	6.29E-07
HALLMARK_EPITHELIAL_MESENCHYMAL_TRANSITION	200	9	0.045	6.09E-06	3.39E-05
HALLMARK_INFLAMMATORY_RESPONSE	200	9	0.045	6.09E-06	3.39E-05
HALLMARK_INTERFERON_GAMMA_RESPONSE	200	9	0.045	6.09E-06	3.39E-05
HALLMARK_APOPTOSIS	161	8	0.0497	9.80E-06	4.90E-05



(caption on next page)

Fig. 3. MT1G mediated BA-induced cell growth inhibition by changing cell cycle distribution in CRC cells. A. Expression analysis of MT1G. After MT1G and control gene corresponding lentivirus infected into CRC cells and MT1G gene stable knock-down or over-expression cell line was screened, cells were treated with BA at indicated concentration for 24 h. The expression of MT1G was measured by RT-PCR. Data are presented as the mean \pm SD, $n = 3$, Student's *t*-test, * $P < 0.05$, ** $P < 0.01$, *** $P < 0.001$, **** $P < 0.0001$. B–C. Analysis of the effects of MT1G on cell proliferation. MT1G gene stable knock-down and over-expression cell line were treated with indicated concentrations of BA for 24 h and then cell viability determined by cck8 were presented as the mean \pm SD, $n = 5$, Student's *t*-test, * $P < 0.05$, ** $P < 0.01$, *** $P < 0.001$, **** $P < 0.0001$. D–E. Analysis of the effects of MT1G on cell cycle distribution. After LV-shMT1G and control lentivirus were infected into CRC cells and MT1G gene stable knockdown cell line was screened, cells were treated with BA at 100 μ M in HT29 and at 80 μ M SW480 cells for 24 h and then cell cycle distribution was determined by Flow Cytometry. The percentages of cells at different periods were generated and statistically analyzed using GraphPad Prism 8 software. Data are presented as the mean \pm SD, $n = 3$, Student's *t*-test, * $P < 0.05$, ** $P < 0.01$, *** $P < 0.001$, **** $P < 0.0001$. F–G. Expression analysis of cell-cycle-related proteins at mRNA levels. RNA was then extracted and the expression of CKD2, CDK4, cyclin D1 and cyclin D3 were determined by RT-PCR. Actin was used as internal control. The expression of these genes was statistically analyzed using GraphPad Prism 8 software. Data are presented as the mean \pm SD, $n = 3$, Student's *t*-test, * $P < 0.05$, ** $P < 0.01$, *** $P < 0.001$, **** $P < 0.0001$. H. Expression analysis of cell-cycle-related proteins at protein levels. Cell proteins were then extracted and the expression of CDK2, CDK4, MT1G, p-Rb and Rb were determined by Western blot. Actin was used as internal control. The full and non adjusted images can be found in supplementary materials named "Full and unadjusted Western blot images".

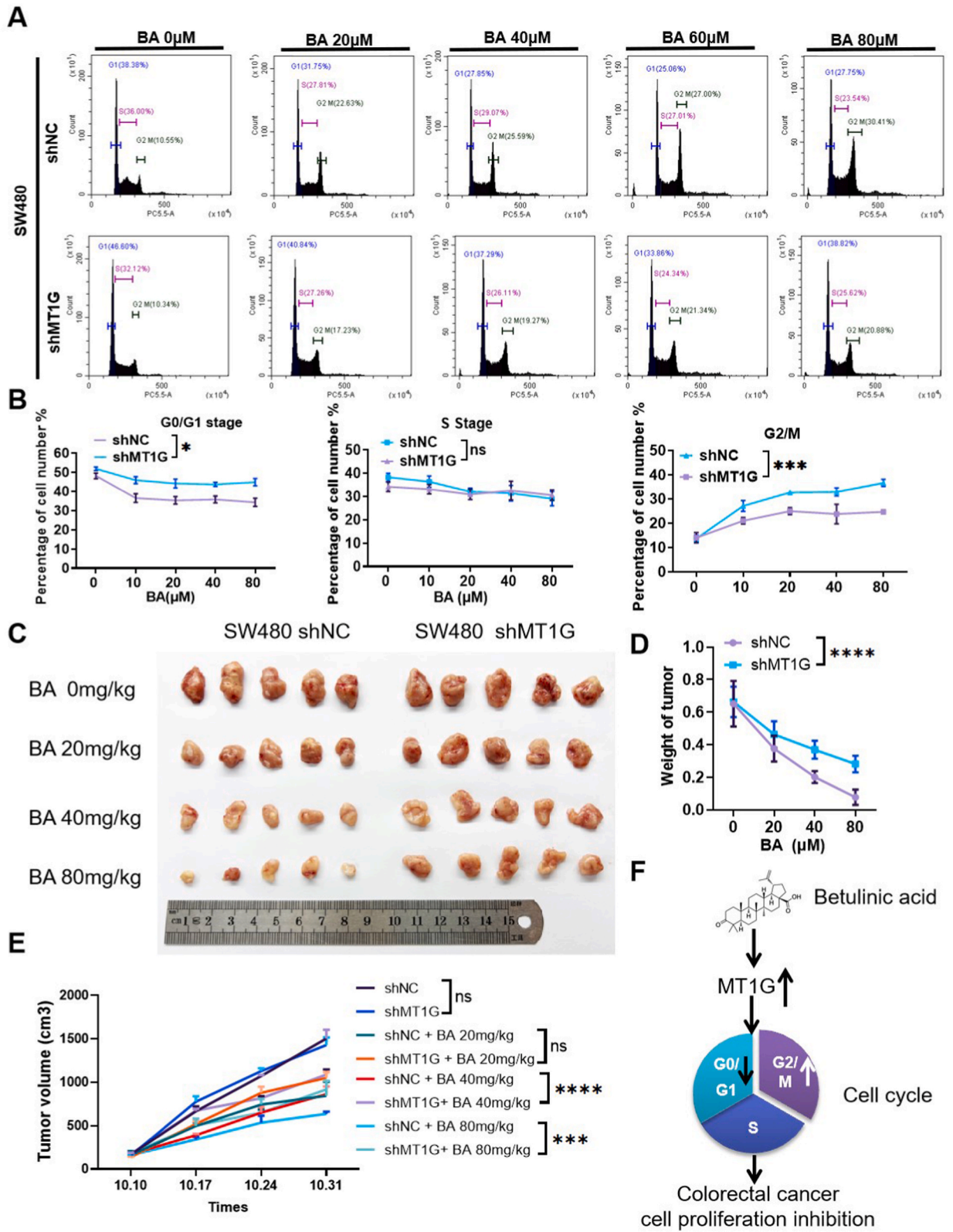
(Supplementary Fig. 1). The list of the top 20 up-regulated and down-regulated overlapping DEGs is shown in Table 1. The reproducibility and repeatability of the results were validated by RT-PCR. The top 6 up-regulated and 6 down-regulated genes of the intersection were selected. As expected, 6 up-regulated genes, MT1G, HSPA6, MT1F, ZNF469, SPRR2D and RGS16, and 6 down-regulated genes, SPTLC3, FAM78A, UBA7, KLRC3, SLC39A10 and TSPOAP1, were further confirmed in BA treatment group vs. control groups in both SW480 and HT29 cells, suggesting that the overlapping genes were trustworthy (Fig. 1E–H).

3.2. BA treatment upregulated the expression of MT1G gene in a dose dependent manner in CRC cells

To better classify the identified overlapping genes, GO enrichment and KEGG analysis of DEGs were implemented. In the cell composition group, DEGs in both SW480 and HT29 cells were mainly enriched in cytoplasm. In the molecular function group, DEGs in both SW480 and HT29 cells were mainly enriched in protein binding. In the biological process group, DEGs in both HT29 and SW480 were mainly enriched in cell cycle (Supplementary Fig. 2A). KEGG analysis revealed DEGs were significantly enriched in mineral absorption, and cell cycle (Fig. 2A). The DEGs induced by BA were involved in mineral absorption, which mainly included MT1 family genes [20]. It is worth noting that MT1G and MT1F were the top 20 significantly DEGs in response to BA and RNA sequencing showed that the expression of all MT1 family genes was also significantly up-regulated by BA in both SW480 cells and HT29 cells, and MT1G had the most obvious fold difference among these genes (Fig. 2B). Next, we further detected the expression changes of MT1G under different concentrations of BA. With increasing BA concentration, the expression of MT1G was up-regulated in a dose-dependent manner in both SW480 and HT29 cells (Fig. 2C). TCGA data analysis showed that MT1G was expressed at lower levels in CRC tissue than in normal colon tissue (Fig. 2D). Additionally, the expression of MT1G in CRC and normal colon tissue was further performed by RT-PCR, and results showed that MT1G was indeed significantly down-regulated in CRC tissues (Fig. 2E). Although, there was no correlation of MT1G expression with TNM stage in colorectal cancer patients (Fig. 2H–J), the results of both survival analysis and disease-free survival analysis showed that the patients with high MT1G expression had longer and higher quality of life than those in the lower expression group (Fig. 2F and G). The above results suggested CRC cell proliferation inhibited by BA, which was previously confirmed by us and others [19,21], was most likely associated with MT1G protein.

3.3. MT1G inhibited the sensitivity of CRC cells to BA by affecting the cell cycle change

To identify the cellular mechanisms by which BA influenced tumor development, we also performed GSEA to compute overlaps between BA-induced 263 DEGs in HT29 and SW480 CRC cells and human MSigDB hallmark gene sets. GSEA analysis revealed BA-induced DEGs had a significant association with G2M_CHECKPOINT and MITOTIC_SPINDLE cell cycle related important pathways (Table 2). To further verify this enrichment result, the association between BA-induced gene sets and CRC was compiled by GSCA. The result showed that BA-induced gene sets in CRC was also significantly enriched in cell cycle (Supplementary Fig. 2B). GO and KEGG analysis indicated that BA induced DEGs was also significantly enriched in cell cycle processes (Supplementary Fig. 2 A and 2A). Due to SW480 cell has lower expression than HT29 cells (Supplementary Fig. 3), the MT1G over-expression lentivirus (OE-MT1G) and control (OE-NC) were used to infect SW480 cells. The MT1G knockdown lentivirus (shMT1G) and control (sh-NC) were used to infect HT29 cells. After the MT1G gene was stably knock down or over-expressed, the over-expression and knockdown effects were determined by RT-PCR (Fig. 3A). Cell proliferation assay showed that MT1G over-expressing cells were more sensitive to BA than the control group (Fig. 3B). While, MT1G knockdown cells had the opposite trend compared to the control (Fig. 3C). To identify whether this phenomenon was dependent on the upregulated MT1G protein, we performed cell cycle assays using MT1G lentiviral stable knockdown cell lines and control cell lines after BA treatment at 100 μ M in HT29 or 80 μ M in SW480. The flow cytometry results showed the proportion of cells in G1 phase reduced, but the proportion of cells in G2/M phase was raised after BA treatment in both HT29 and SW480 cells compared to the control DMSO treatment in shNC-SW480 cells, in contrast, MT1G knockdown partially reversed this phenomenon (Fig. 3D and E). We observed that the mRNA levels of CDK2, CDK4, cyclin D1 and cyclin D3 were significantly up-regulated after BA treatment compared to the control in HT29 cells, while CDK2, CDK4, and cyclin D3 proteins were significantly



(caption on next page)

Fig. 4. MT1G knockdown restrained BA-induced cell growth inhibition by changing cell cycle distribution in CRC cells in a dose dependent manner in vivo. A. Cell cycle distribution induced by different concentrations of BA after MT1G or NC gene knockdown. After LV-shMT1G and control lentivirus were infected into SW480 cells and MT1G gene stable knockdown cell line was screened. These cells were treated with BA at 20 μ M, 40 μ M, 60 μ M, 80 μ M in SW480 cells for 24 h, respectively, and then cell cycle distribution was determined by Flow Cytometry. The percentages of cells at different periods were generated and statistically analyzed using GraphPad Prism 8 software. Data are presented as the mean \pm SD, n = 3, Two way ANOVA test, * P < 0.05, ** P < 0.01, *** P < 0.001, **** P < 0.0001. B. Exhibition of the growth of subcutaneous tumors induced by BA with different concentrations after MT1G or NC gene knockdown. After LV-shMT1G and control lentivirus were infected into SW480 cells and MT1G gene stable knock-down and control cells were subcutaneously injected at the left axilla of the nude mice for 1 week and then mice were injected intraperitoneally with 20 mg/kg/day, 40 mg/kg/day or 80 mg/kg/day of BA. C. Tumor weights were measured and analyzed in shMT1G and shNC groups. Data are presented as the mean \pm SD, n = 3, Two way ANOVA test, * P < 0.05, ** P < 0.01, *** P < 0.001, **** P < 0.0001. D. Tumor volume were measured and analyzed in shMT1G and shNC groups. Tumor length and width were measured every 7 days, mice were sacrificed at day 30, subcutaneous tumors were dissected, photographed, and weighed. Data are presented as the mean \pm SD, n = 3, Two way ANOVA test, * P < 0.05, ** P < 0.01, *** P < 0.001, **** P < 0.0001. E. Mechanism summary diagram. BA induced colorectal cancer cell cycle alterations in G0/G1 and G2/M phase via upregulating MT1G proteins, which leads to inhibition of CRC cells proliferation.

up-regulated in SW480 cells. MT1G gene knockdown significantly offset the BA-induced increase of CDK2 and CDK4 protein expression compared to that in the control group at the mRNA level in both HT29 and SW480 cells (Fig. 3F and G). p-Rb/Rb plays an important role in cell cycle conversion [22], and the expression of p-Rb and Rb was also further detected by Western blot. The results showed BA augmented the expression of CDK2, CDK4 and p-Rb at the protein levels and this phenomenon was also damaged by MT1G knockdown (Fig. 3H), suggesting that MT1G has an indispensable role in the induction of cell cycle progression alteration by BA treatment.

3.4. MT1G knockdown restrained BA-induced cell growth inhibition by changing cell cycle distribution in a dose dependent manner in vivo

To further identify that the cell cycle changes induced by BA were influenced by the expression of MT1G in a dose-dependent manner, we therefore further performed concentration gradient experiments in shMT1G and shNC groups to analyze the cell cycle changes induced by different concentrations of BA. The results of cell cycle analysis showed that with the increase of BA concentration, the proportion of cells in G0/G1 phase decreased and the proportion of G2/M phase cells increased successively in shNC-SW480 cells; however, in shMT1G-SW480 cells, the proportion of cells in G0/G1 and G2/M phase kept almost unchanged with the increase of BA concentration (Fig. 4A). To verify this in vivo, we injected mice with the same number of shNC-SW480 and shMT1G-SW480 cells subcutaneously and intraperitoneally injected with different doses of BA or DMSO a week later. Results displayed BA significantly inhibited the tumor growth in a concentration-dependent manner in shNC-SW480 group, whereas in tumors formed by shMT1G-SW480 cells, BA slightly inhibited the tumor growth (Fig. 4B–E). Above results showed MT1G promoted BA-induced cell cycle changes in CRC cells both in vitro and in vivo, and then inhibited CRC cells proliferation.

4. Discussion

Colorectal cancer is one of the most malignant cancers in the world [1]. High mortality rates demonstrate growing interest in identifying novel high-potency and TCMS related pharmacological agents of cancer treatment [23]. BA is a naturally occurring pentacyclic triterpenoid from plant origin and has been noticed recently for its antitumor effect [24]. Nevertheless, we and others reported that BA suppressed the growth of tumor cells in CRC cells [25], and their potential targets in CRC based on RNA sequencing have not been systematically studied.

RNA sequencing has many advantages for unbiased detection of transcripts as well as low-abundance transcripts [26]. Therefore, bioinformatics methods were used to identify the central DEGs of CRC cells induced by BA. Our study finds for the first time that BA inhibits CRC proliferation by enhancing the mineral absorption pathway by GO and KEGG analysis. The absorption of minerals is mainly regulated by metallothionein (MTs). In 1957, MTs were found to be responsible for the metabolism of naturally accumulated tissue components in mammalian kidneys [27] and were known as sulfhydryl rich proteins [28]. In humans, MTs has four major subtypes (MT1, MT2, MT3, MT4), which encodes genes on chromosome 16q13 (29) [11]. Emerging evidence indicates that MTs play an important role in tumorigenesis, progression and drug resistance [27]. MT1G is expressed at lower levels in CRC cells than in normal tissues. In addition, gene signature including MT1G predicted the survival rate [28]. High MT1G isoform expression sensitizes colon cells to oxaliplatin and 5-fluorouracil [29]. Consistently, our results showed that MT1G overexpressing cells were more sensitive to BA than control cells. MT1G knockdown cells had the opposite trend compared to the control. The MT1G protein is sulfhydryl rich proteins with high affinity for binding a variety of copper ions. Copper is also a very important allosteric modulator of enzymes, such as mitogen-activated protein kinase 1 (MEK 1) and MEK 2 in cell growth and proliferation [30]. Therefore, we speculated that BA most probably increased the binding of cells to copper ions by activation of MT1G protein, resulting in the decreased activity of cell proliferation-related protein kinase, and subsequent inhibiting colorectal cancer cell proliferation. The above results were further prompt us that BA can function as an effective chemotherapeutic agent, such as OXA and 5-FU, to kill CRC through MT1G regulation.

The cell cycle was divided into G1/G0, S, G2/M stages. Cells are driven through these stages by cyclin-dependent kinases (CDKs) and their partner cyclins. CDKs (e.g., CDK2 and CDK4) sequentially regulate various events of the cell-cycle. Among them, G1 is directly regulated by CDK2 and CDK4 [31]. The CDK4 and CDK2 contributes to control cell cycle entry and phosphorylates

retinoblastoma protein (pRb), causing a transition of cell-cycle from G to S phase [32]. MT1G over-expression increased the number of cells in G1 phase and decreased the number of cells in S and G2 phases in NCI-N87 and HGC-27 cells [12]. In addition, the cell cycle was also arrested at the G1 phase when cells were over-expressed with MT1G gene, with the number of G1 phase cells increasing approximately 7 % in K1 cells and FTC133 cells [33]. Another study reported that high MT1G expression weakens ATRA-induced G1 arrest in NB4 cells by regulating the induction of the G1 regulator [34]. Our results confirmed that BA treatment significantly reduced the number of cells in G1 phase and increased G2 phase in CRC cells. Mechanistically, BA altered the cell cycle distribution accompanied by increased expression of CDK2, CDK4, and much more retinoblastoma protein (pRb) in the phosphorylation state in HT29 and SW480 cells, while MT1G knockdown impaired the BA-induced augmentation of CDK2, CDK4 and p-RB. These results indicated that MT1G mediates BA to arrest the cell cycle at G2/M phase through CDK2 and CDK4, which keeps retinoblastoma protein (pRb) in phosphorylation state. Most importantly, we enriched BA-induced differential genes through GSEA and GSCA, and BA-induced DEGs were enriched into G2/M cycle transition and cell cycle process, which is consistent with our functional experiment that BA-induced G2/M cell arrest through MT1G regulation. This phenomenon was further verified by concentration gradient experiments and in vivo nude mice, so we summarized the involvement of MT1G in the altered cell cycle progression induced by BA treatment.

In conclusion, we found that BA significantly upregulated the expression of MT1G and affected the cell cycle proceeding by upregulating MT1G, in order to inhibit CRC cell proliferation, providing a theoretical basis for the clinical treatment of BA in the future.

Ethical statement

The study was conducted in accordance with the protocol approved by the Ethics Committee of the Affiliated Hospital of Jining Medical College (2022B060) and good clinical practice guidelines.

Data availability statement

The datasets presented in this study can be found in online repositories. The name of the repository was Genome Sequence Archive-Human and accession number can be found below: HRA006023.

CRedit authorship contribution statement

Yuqin Zhang: Resources. Xiaxia Yang: Resources. sen wang: Writing – original draft, Project administration, Methodology, Investigation, Funding acquisition, Formal analysis, Data curation, Conceptualization. Bao gui Zhang: Resources, Formal analysis. Bin Zhang: Writing – review & editing, Supervision. Kexin Wang: Methodology. Xiao Yang: Resources, Formal analysis. Qingli Bie: Writing – review & editing

Informed consent from the patient to allow the use of his sample

Authorization Letter of Affiliated Hospital of Jining Medical College.

I solemnly authorize the above-mentioned agent to act as my agent during this hospitalization, exercising my medical informed consent on my behalf. The right to choose, sign relevant informed consent forms, and choose whether to assume corresponding medical risks. The signature of the authorized agent shall be deemed as the signature of the principal, and any consequences arising from the signing of the informed consent form shall be borne by the principal. The above agents are all separate agents.

The authority of an agent includes but is not limited to the following:

1. Understand my condition, diagnosis and treatment plan, medical risks, medical expenses, etc., and make choices about my diagnosis and treatment plan;

2. When surgery, anesthesia, special examinations/treatments (such as invasive diagnosis and treatment procedures, use of medical insurance payment items, implanted materials, etc.) are required, clear and definite opinions should be written on the relevant informed consent form and signed;

3. Understand whether the drugs and medical devices received are clinical trials and other medical research projects, and choose whether to participate;

4. Protect personal privacy rights, etc.

1#Patient Name: Zhaokun Qiu. Gender: Male. Age: 89 years old. Department: Digestive Medicine Ward 1 (Taibai Lake). ID number: 7101252297. Medical record number: 1851806.

2#Patient Name: Qingtong Fan. Gender: Male. Age: 68 years old. Department: Gastrointestinal Surgery Colorectal Group 1. ID number: 7100966027. Medical record number: 1827617.

3#Patient Name: Peiliang Li. Gender: Male. Age: 82 years old. Department: Gastrointestinal Surgery Colorectal Ward. ID number: 7101541152. Medical record number: 1825166.

4#Patient Name: Yumei Liu. Gender: Female. Age: 59 years old. Department: Gastrointestinal Surgery Colorectal Ward. ID number: 7101464208. Medical record number: 1817923.

5#Patient Name: Yucheng Lu. Gender: Male. Age: 74 years old. Department: Thoracic Surgery Ward. ID number: 7101547027. Medical record number: 1826189.

6# Patient name: Yumin Su. Gender: Male. Age: 64 years old. ID number: 7101540293.

Medical record number: 1825052.

7#Patient Name: Xianling Wei. Age:78 years old. Gender: Female. Department: Gastrointestinal Surgery Ward. ID number: 7100981740. Medical record number: 1722309.

8#Patient Name: Yunfu Wu. Age:75 years old. Gender: Male. Department: Gastrointestinal Surgery Ward. ID number: 7101193409. Medical record number: 1762583.

9#Patient Name: Jian Zhang. Age:51 years old. Gender: Male. Department: Gastrointestinal Surgery Ward. ID number: 3002034308. Medical record number: 1837350.

10#Patient Name: Maoting Zhang. Gender: Male. Age: 65 years old. Department: Digestive Tumor Ward. ID number: 7101498229. Medical record number: 1823170.

11#Patient name: Qingzhe Zhang. Gender, Male. Age, 70 years old. Department: Gastrointestinal Surgery Colorectal Ward. ID number: 7101482875. Medical record number: 1821251.

12#Patient Name: Xiqiang Zhen. Gender: Male. Age: 65 years old. Department: Pelvic Tumor Ward. ID number: 7101531780. Medical record number: 1824715.

Declaration of competing interest

The authors declare that they have no known competing financial interests or personal relationships that could have appeared to influence the work reported in this paper.

Acknowledgements

We are grateful to all patients who participated in this research and thanks for supports from the below fundings. This study was supported by grants from the National Natural Science Foundation of China (No. 82102798,82173371,82273447,82273069,82372679), Post-doctoral Program of Affiliated Hospital of Jining Medical College, the China Postdoctoral Science Foundation (No.2022M721339), Shandong Traditional Chinese Medicine Science and Technology Project (No.M – 2022244), Tai Shan Young Scholar Foundation of Shandong Province (No. tsqn201909192), Shandong Provincial Natural Science Foundation (No. ZR2019BH050, ZR2020YQ59.), PhD Research Foundation of the Affiliated Hospital of Jining Medical University (No. 2020-BS006), Academician He Lin Fund of Jining Medical College (No. JYHL2019FMS05).

Appendix A. Supplementary data

Supplementary data to this article can be found online at <https://doi.org/10.1016/j.heliyon.2023.e23833>.

References

- [1] J. Luo, et al., miR5765p promotes epithelial to mesenchymal transition in colorectal cancer by targeting the Wnt5a mediated Wnt/betacatenin signaling pathway, *Mol. Med. Rep.* 23 (2) (2021).
- [2] S.G. Patel, et al., The rising tide of early-onset colorectal cancer: a comprehensive review of epidemiology, clinical features, biology, risk factors, prevention, and early detection, *Lancet Gastroenterology & Hepatology* 7 (3) (2022) 262–274.
- [3] J.X. Li, et al., Genetic and biological hallmarks of colorectal cancer, *Gene Dev.* 35 (11–12) (2021) 787–820.
- [4] K.C. Wu, et al., Development of a traditional Chinese medicine-based agent for the treatment of cancer cachexia, *Journal of Cachexia Sarcopenia and Muscle* 13 (4) (2022) 2073–2087.
- [5] X.L. Zhang, et al., Polyphenol from millet bran increases the sensitivity of colorectal cancer cells to oxaliplatin by blocking the ganglioside GM3 catabolism, *Food Funct.* 12 (1) (2021) 291–301.
- [6] D. Gheorgheosu, et al., Betulinic acid as a potent and complex antitumor phytochemical: a minireview, *Anti Cancer Agents Med. Chem.* 14 (7) (2014) 936–945.
- [7] L. Jiao, et al., Betulinic acid suppresses breast cancer aerobic glycolysis via caveolin-1/NF- κ B/c-Myc pathway, *Biochem. Pharmacol.* 161 (2019) 149–162.
- [8] S. Amiri, et al., Betulin and its derivatives as novel compounds with different pharmacological effects, *Biotechnol. Adv.* 38 (2020).
- [9] J. Chen, et al., Betulinic acid enhanced the chemical sensitivity of esophageal cancer cells to cisplatin by inducing cell pyroptosis and reducing cell stemness, *Ann. Palliat. Med.* 9 (4) (2020) 1912–1920.
- [10] L.A. Weber, et al., Betulinic acid shows anticancer activity against equine melanoma cells and permeates isolated equine skin in vitro, *BMC Vet. Res.* 16 (1) (2020).
- [11] M.G. Cheria, A. Jayasurya, B.H. Bay, Metallothioneins in human tumors and potential roles in carcinogenesis, *Mutat Res* 533 (1–2) (2003) 201–209.
- [12] G. Xu, et al., MT1G inhibits the growth and epithelial-mesenchymal transition of gastric cancer cells by regulating the PI3K/AKT signaling pathway, *Genet. Mol. Biol.* 45 (1) (2022), e20210067.
- [13] F.B. Mullauer, et al., Betulinic acid delivered in liposomes reduces growth of human lung and colon cancers in mice without causing systemic toxicity, *Anti Cancer Drugs* 22 (3) (2011) 223–233.
- [14] B. Peng, et al., Ferroptosis-related gene MT1G as a novel biomarker correlated with prognosis and immune infiltration in colorectal cancer, *Front. Cell Dev. Biol.* 10 (2022), 881447.
- [15] N.M.G. de Couto, et al., Betulinic acid and brosimine B hybrid derivatives as potential agents against Female cancers, *Anti Cancer Agents Med. Chem.* 20 (5) (2020) 622–633.
- [16] C. Fang, et al., Assessment of the cPAS-based BGISEQ-500 platform for metagenomic sequencing, *GigaScience* 7 (3) (2018) 1–8.
- [17] P.J. Cock, et al., The Sanger FASTQ file format for sequences with quality scores, and the Solexa/Illumina FASTQ variants, *Nucleic Acids Res.* 38 (6) (2010) 1767–1771.
- [18] S. Audic, J.M. Claverie, The significance of digital gene expression profiles, *Genome Res.* 7 (10) (1997) 986–995.
- [19] S. Wang, et al., Overaccumulation of P53-Mediated Autophagy Protects against Betulinic Acid-Induced Apoptotic Cell Death in Colorectal Cancer Cells, vol. 8, *Cell Death & Disease*, 2017.

- [20] P. Chawla, et al., Improvement of mineral absorption and nutritional properties of seeds using solid-state fermentation, *J. Am. Coll. Nutr.* 39 (7) (2020) 628–635.
- [21] G. Wang, et al., The antitumor activity of betulinic acid-loaded nanoliposomes against colorectal cancer in vitro and in vivo via glycolytic and glutaminolytic pathways, *J. Biomed. Nanotechnol.* 16 (2) (2020) 235–251.
- [22] N. Geng, et al., [Aldo-keto reductase family 1 B10 participates in the regulation of hepatoma cell cycle through p27/p-Rb signaling pathway], *Zhonghua Gan Zang Bing Za Zhi* 28 (10) (2020) 861–867.
- [23] E. Cretu, et al., Plant-derived anticancer agents - curcumin in cancer prevention and treatment, *Rev. Med.-Chir. Soc. Med. Nat. Iasi* 116 (4) (2012) 1223–1229.
- [24] H.F. Wang, et al., Betulinic acid induces apoptosis of gallbladder cancer cells via repressing SCD1, *Acta Biochim. Biophys. Sin.* 52 (2) (2020) 200–206.
- [25] A.Q. Zeng, et al., Betulinic acid induces apoptosis and inhibits metastasis of human colorectal cancer cells in vitro and in vivo, *Bioorg. Med. Chem.* 27 (12) (2019) 2546–2552.
- [26] R.D. Hawkins, G.C. Hon, B. Ren, Next-generation genomics: an integrative approach, *Nat. Rev. Genet.* 11 (7) (2010) 476–486.
- [27] J.H. Kagi, Overview of metallothionein, *Methods Enzymol.* 205 (1991) 613–626.
- [28] N. Thirumoorthy, et al., Metallothionein: an overview, *World J. Gastroenterol.* 13 (7) (2007) 993–996.
- [29] J.M. Arriaga, et al., Metallothionein expression in colorectal cancer: relevance of different isoforms for tumor progression and patient survival, *Hum. Pathol.* 43 (2) (2012) 197–208.
- [30] P. Tsvetkov, et al., Copper induces cell death by targeting lipoylated TCA cycle proteins, *Science* 375 (6586) (2022) 1254–1261.
- [31] T.A. Chohan, et al., An insight into the emerging role of cyclin-dependent kinase inhibitors as potential therapeutic agents for the treatment of advanced cancers, *Biomed. Pharmacother.* 107 (2018) 1326–1341.
- [32] S.H. Lim, P. Kaldis, Cdks, cyclins and CKIs: roles beyond cell cycle regulation, *Development* 140 (15) (2013) 3079–3093.
- [33] J. Fu, et al., Metallothionein 1G functions as a tumor suppressor in thyroid cancer through modulating the PI3K/Akt signaling pathway, *BMC Cancer* 13 (2013).
- [34] N. Hirako, H. Nakano, S. Takahashi, A PU.1 suppressive target gene, metallothionein 1G, inhibits retinoic acid-induced NB4 cell differentiation, *PLoS One* 9 (7) (2014).